CYP51 from *Trypanosoma brucei* Is Obtusifoliol-Specific[†]

Galina I. Lepesheva,*,[‡] W. David Nes,[§] Wenxu Zhou,[§] George C. Hill,[‖,⊥] and Michael R. Waterman[‡]

*Department of Biochemistry, Vanderbilt University School of Medicine, Nashville, Tennessee 37232-0146,
Department of Chemistry and Biochemistry, Texas Tech University, Lubbock, Texas 79409-1061, Department of Microbiology,
Meharry Medical College, Nashville, Tennessee 37208-3599, Department of Microbiology,
Vanderbilt University School of Medicine, Nashville, Tennessee, 37232-0146*

ABSTRACT: New isoforms of CYP51 (sterol 14α-demethylase), an essential enzyme in sterol biosynthesis and primary target of azole antimycotic drugs, are found in pathogenic protists, *Trypanosoma brucei* (TB), *T. vivax, T. cruzi,* and *Leishmania major.* The sequences share ~80% amino acid identity and are ~25% identical to sterol 14α-demethylases from other biological kingdoms. Differences of residues conserved throughout the rest of the CYP51 family that align with the BC-loop and helices F and G of CYP51 from *Mycobacterium tuberculosis* (MT)) imply possible alterations in the topology of the active site cavity of the protozoan enzymes. CYP51 and cytochrome P450 reductase (CPR) from TB were cloned, expressed in *Escherichia coli,* and purified. The P450 has normal spectral features (including absolute absorbance, carbon monoxide, and ligand binding spectra), is efficiently reduced by TB and rat CPR but demonstrates altered specificity in comparison with human CYP51 toward three tested azole inhibitors, and contrary to the human, *Candida albicans,* and MT isoforms, reveals profound substrate preference toward obtusifoliol (turnover 5.6 min^{-1}). It weakly interacts with the other known CYP51 substrates; slow lanosterol conversion predominantly produces the 14α-carboxyaldehyde intermediate. Although obtusifoliol specificity is typical for plant isoforms of CYP51, the set of sterol biosynthetic enzymes in the protozoan genomes together with available information about sterol composition of kinetoplastid cells suggest that the substrate preference of TBCYP51 may reflect a novel sterol biosynthetic pathway in Trypanosomatidae.

Sterol biosynthesis is one of the general metabolic pathways present in the majority of eukaryotic cells and organisms. It leads to production of cholesterol in animals, ergosterol in fungi, and a variety of phytosterols in plants. The sterols are predominantly used to build membranes but also serve as precursors of steroid hormones and phytohormones (*1−3*). While the initial part of sterol biosynthesis (between acetoacetyl CoA and squalene 2,3-epoxide) is general in eukaryotic cells, at the stage of squalene 2,3-epoxide cyclization, the pathway is known to bifurcate into two branches. Being cyclized by lanosterol synthase (EC 5.4.99.7), in animals and fungi squalene 2,3-epoxide forms lanosterol (LS),[1] which further can be either hydrogenated into 24,25-dihydrolanosterol (DHL) (animals) or methylated into 24-methylene-24,25-dihydrolanosterol (MDL) (filamentous fungi) (Supporting Information). In plants and algae,

squalene 2,3-epoxide cyclization produces cycloartenol; the reaction is catalyzed by cycloartenol synthase (EC 5.4.99.8). The following conversion of cycloartenol includes consecutive 24-methylation and removal of the angular (β-) methyl group at position 4 leading to formation of obtusifoliol. LS, DHL, MDL, and obtusifoliol are all substrates of sterol 14α-demethylase (CYP51), the only cytochrome P450 family having catalytically identical orthologs in different biological kingdoms (*4, 5*). Although sterol biosynthetic pathways in prokaryota are not known, several enzymes with sterol 14α-demethylase (14α-DM) activity are found in bacteria (e.g., *Mycobacterium tuberculosis* (MT), *M. smegmatis, M. avium,* and *Methylococcus capsulatus*).

The catalytic cycle of 14α-DM consists of three successive stereospecific monooxygenations, including conversion of the sterol 14α-methyl group into 14α-hydroxymethyl and 14α-carboxyaldehyde derivatives followed by loss of formic acid and conjugated $\Delta^{14,15}$ double bond formation (*6*). Detailed studies of the mechanism of the reaction have shown that under certain in vitro conditions 14α-hydroxymethyl and 14α-carboxyaldehyde intermediates can be accumulated in the mixture (*7−9*). In vivo accumulation of 14α-carboxyaldehyde derivative of LS is known to down-regulate

* To whom the correspondence should be addressed. Mailing address: Department of Biochemistry, Vanderbilt University School of Medicine, 622 Robinson Research Bldg., 23rd and Pierce Avenues, Nashville, TN 37232-0146. Tel: 615-322-3318. Fax: 615-322-4349. E-mail: galina.i.lepesheva@vanderbilt.edu.

[‡] Department of Biochemistry, Vanderbilt University School of Medicine.
[§] Texas Tech University.
[‖] Meharry Medical College.
[⊥] Department of Microbiology, Vanderbilt University School of Medicine.

[1] Abbreviations: CYP, cytochrome P450 gene or protein; CYP51 of 14α-DM, sterol 14α-demethylase; CPR, cytochrome P450 reductase; LS, lanosterol; DHL, 24,25-dihydrolanosterol; MDL, 24-methylene DHL; HPCD, 2-hydroxypropyl-β-cyclodextrin; TB, *Trypanosoma brucei*; MT, *Mycobacterium tuberculosis.*

```
                                                                                                          αA'      αA
                                                                                                       ϙϙϙϙϙϙ ϙϙϙϙϙϙ
                                                                                                         .
MT          1  ...................................................MSAVALPRVSGGHDEHGHLEEFRTDPIGLMQ
Human       1  MLLLGLLQAGGSVLGQAMEKVTGGNLLSMLLIACAFTLSLVYLIRLAAGHLVQ...LPAGVKSPPYIFSPIPFLGHAIAFGKSPIEFLE
T.brucei    1  ............................................MLLEVAIFLLTALALYSFYFVKSFNVTRPTDFPVYPVTVFILGHIIQFGKSPLGFMQ
T.vivax     1  ............................................MLLEVITFLLTVLVLYSVYFVVSFNVTRPTDFPVRHVALFFLGHIIPFGKDPLGFML
T.cruzi     1  ............................................MFIEAIVLALTALILYSVYSVKSFNTTRPTDFPVYPVTVFPLGHIVQFGKNPLEFMQ
Leishmania  1  ............................................MIGRFFLLLTAGLALYGWYFCKSFNTTRPTDFPVVHGAMLFVGHILIQFGKDPLDFML

               β1-1        β1-2           αB           β1-5          αB'                    αC
               ϙϙϙϙϙϙ  →     →         ϙϙϙϙϙϙϙϙ          TT     ϙϙϙϙϙϙ           ϙϙϙϙϙϙϙϙ            ϙϙϙϙϙϙϙϙ
                           TT                                      .
MT         32  RVRDECG.DVGTFQLAGKQVVLLSGSHANEFFFRAGDDDLDQAKAY.PFMTPIFGEGVVFDAS.PERRKEMLHN.AALRGEQMKGHAA
Human      87  NAYEKYG.PVFSFTMVGKTFTYLLGSDAAALLFNSKNEDLNAEDVYSRLTTPVFGKGVAYDVPNPVFLEQKMLKSGLNIAHFKQHVS
T.brucei   58  ECKRQLKSGIFTINIVGKRVTIVGDPHEHSRFLPRNEVLSPREVY.SFMVPVFGSGVVAYAAPYPRMREQLNFLAEHLIIAKFQNFVP
T.vivax    58  ECKRKLRSGVFTINIMGKRVTVVGDPREHSRFLPRNEVLSPREVY.AFMVPVFGSGVAYAAPYPRMREQLNFLAEHLIIAKFQNFVP
T.cruzi    58  RCKRRELKSGVFTISIGGQRVTIVGDPHEHSRFLSPRNEILSPREVY.TIMTPVFGSGVAYSAPYPRMREQLNFLAEHLIIAKFQNFVP
Leishmania 58  NAKKKYG.GVFTMNICGNRVTVVGDVHQHNKFFTPRNEILSPREVY.SFMVPVFGSGVAYAAPYPRMREQLNFLAEHLLVAKFQNEAP
                                                                       ↑ SRS1

               αD              β3-1          αE                  αF'           αF              αF"
               ϙϙϙϙϙϙϙϙϙϙ                  → ϙϙϙϙϙϙϙϙϙϙϙϙϙϙϙ          ϙϙϙϙ  ϙ.ϙϙϙϙϙϙϙϙϙϙ   ϙϙϙϙ            ϙϙϙϙϙϙϙϙ
                     .
MT        116  TIEDQVRRMIA.DWG.EAGEIDLLDFFAELTIYTSSACLIGKKFRDQLDG.RFAKLYHELERGTDPLAYVDP...YLPIESFRRRDEA
Human     174  IIEKETKEYFESWG..ESGEKNVFEALSELIILTASHCLHGKEIRSQLNE.KVAQLYADLDGGFSHAAWLLPG..WLPLPSFRRRDRA
T.brucei  145  ATQHEVRKFMAANWDKDEGEINLLEDCSTMIINTACQCLIGEDLRKRLDARRFAQLLAKMESSLIPAAVFLPILLKLPLPQSARCHEA
T.vivax   145  ATQHEARKFLSENWNKDEGQVNLLEDCSAMIINTACQCLIGEDLRKRLDARRFAQLLAKMESSLIPAAVFMPSLLLLPLPQSACCRDA
T.cruzi   145  ATQHEVRKFMAENWKKDEGVINLLEDCSAMIINTACQCLIGEDLRKRLNARHFAQLLSKMESSLIPAAVFMPWLLRLPLPQSARCREA
Leishmania144  STQHEVRKFMKANWNKDEGEINILDDCSAMIINTACQCLIGEDLRKRLDARQFAQLLAKMESCLIPAAVFLPWILKLPLPQSYRCRDA
                                                              SRS2                            SRS3

               αG                           αH                              αI                           αJ
               ϙϙϙϙϙϙϙϙϙϙϙϙϙ              ϙϙϙϙϙϙϙ    TT     ϙϙϙϙϙϙϙϙϙϙϙϙϙϙϙϙϙϙϙϙϙ ϙϙϙϙϙϙϙϙϙϙϙϙ   ϙϙϙϙϙϙ
                      .
MT        198  RNGLVALVADIMNGRIANPPTDKSD.RDMLDVLIAVKAETGTPRFSADEITGMFISMMFAGHHTSSGTASWTLIELMRHRDAYAAVID
Human     257  HREIKDIFYKAIQKRRQSQ..EKID..DILQTLLDATYKDGRP.LTDDEVAGMLIGLLLAGQHTSSTTSAWMGFFLARDKTLQKKCYL
T.brucei  233  KTELQKILSEIIARKEEBVNKDSSTSDLLSGLLSAVYRDGTP.MSLHEVCGMIVAAMFAGQHTSSITTIWWMLHLMHRANVKHLEAL
T.vivax   233  REELQLILSEIIILARKREEVNKDSGTSDLLSGLLSAVYRDGTP.MSLHEVCGMIVAAMFAGQHTSSITTIWWMLHLMHRANVKHLETL
T.cruzi   233  RAELQKILGEIIVAREKEEASKDNNTSDLLGGLIKAVYRDGTR.MSLHEVCGMIVAAMFAGQHTSTITTIWWSMLHLMHRKNKKWLDKL
Leishmania232  RAELQDILSEIIIAREKEEAQKDSNTSDLLASLIGAVYRDGTR.MSQHEVCGMIVAAMFAGQHTSTITTIWWSLLHLMDRRNKRHLAKL
                                                                      SRS4

               αJ'          αK                      β1-4    β2-1  β2-2    β1-3   αK'                   3₁₀K'''
               ϙϙϙϙϙϙϙ    ϙϙϙϙ         ϙϙϙϙϙ.ϙϙϙϙϙϙ     →        →   →        →   ϙϙϙϙ       TT     ϙϙϙ
                     .                                              TT      TT                          .
MT        285  ELDELYGDGR.SVSFHALRQIPQLEN.VLKETLRLHPPLIILMRVAKGEFEVQGHRIHEGDLVAASPAISNRIPEDFPDPHDFVPARY
Human     340  EQKTVCGENLPPLTYDQLKDLNLLDR.CIKETLRLRPPIMIMMRMARTPQTVAGYTIPPGHQVCVSPTVNQRLKDSWVERLDFNPDRY
T.brucei  320  RKEIBEFPAQ..LNYNNVMDEMPFAERCARESIRDPPLLMLRKVMADVKVGSYVVPKGDIIACSPLLSHHDEAFPEPRRWDPERD
T.vivax   320  RKEIEEFPAQ..LNYSNVMDEMPFAERCARESIRDPPLIMLRKVLADVKVGSYVVPKGDIIACSPLLSHHDEAFPDPRRWDPERE
T.cruzi   320  HKEIDEFPAQ..LNYDNVMDEMPFAERCVRESIRDPPLLMVVRMVKAEVKVGSYVVPKGDIIACSPLLSHHDEAFPNPRLWDPERD
Leishmania319  HQEIDEFPAQ..LNYDNVMEEMPFAEQCARESIRDPPLIMLWRKVLKPVQVGKCVVPEGDIIACSPLLSHQDEEAFPNPREWNPERN
                                                   SRS5

               αK"                      αL         β3-3          β4-1     β4-2     β3-2
               ϙϙϙϙ      TT    ϙϙϙ    ϙϙϙϙϙϙϙϙϙϙϙϙϙϙϙϙϙϙϙϙϙϙ →      ϙϙϙ      →        →       →
                     .
MT        371  EQPRQEDLLNRWTWIPFGAGRHRCVGAAFAIMQIKAIFSVLLREYEFEMAQPPESYRNDHSKMVVQLAQPACVRYRRRTGV..
Human     427  LQDNP.ASGEKFAYVPFGAGRHRCIGENPAYVQIKTIWSTMLRLYEFDLIDGYFPTVN.YTTMIHTPENPV.IRYKRRSK...
T.brucei  406  EK.......VEGAFIGFGAGVHKCIGQKFGLLQVKTILATAFRSYDFQLLRDEVPDPDYHTMVVGPTASQCRVKYIRRKAAAA
T.vivax   406  EV.......IEGAFIGFGAGVHKCIGQKFGLLQVKTILATVLRDYDFELPRDEVPEPDYHTMVVGPTSSQCRVRMIRRKKPAS
T.cruzi   406  EK.......VDGAFIGFGAGVHKCIGQKFALLQVKTILATAFREYDFQLLRDEVPDPDYHTMVVGPTLNQCLVKMTRKK....
Leishmania405  MKL......VDGAFCFGAGVHKCIGEKFGLLQVKTVLATVLRDYDFELLG.PLPEPNYHTMVVGPTASQHCRVKYIRKKAAA.
                                                                       SRS6
```
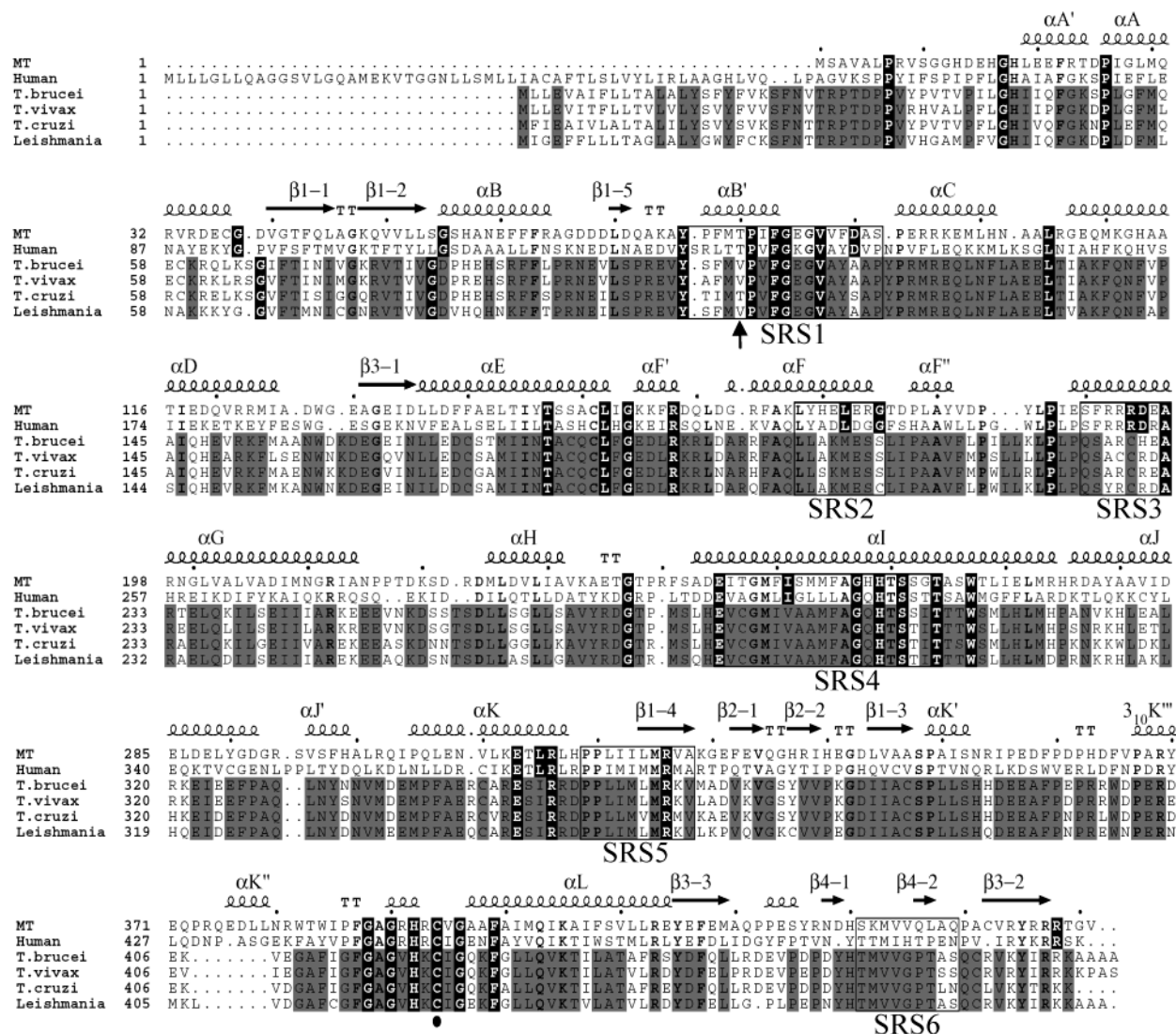
FIGURE 1: Alignment of sterol 14α-DM from Trypanosomatidae genomes. Assignment of secondary structural elements is based on the MTCYP51 structure (PDB entry 1E9X). The residues conserved in the sequences from Trypanosomatidae are shaded in gray. The residues conserved throughout the sequences of CYP51 from animals, plants, fungi, and bacteria are shaded in black. Shifted location of two glycines (G38 and G55 in MTCYP51) is likely to indicate slight alterations in the length of helices A and B in the protozoan sequences. The six P450 SRSs (*53*) are framed and numbered. The heme-coordinated cysteine is marked with black circle below the alignment. Location of a single amino acid difference (V107) from the sequence in the NCBA database found in the clone of TB used in this study is shown with an arrow.

cholesterol biosynthesis by posttranscriptional modulation of 3-hydroxy-3-methylglutaryl-CoA reductase activity (*10−12*).

The reaction of 14α-DM is highly sensitive to azole inhibitors (*13*), interaction of a basic nitrogen with the P450 heme iron preventing substrate binding and metabolism. Blocking of sterol 14α-DM is lethal in yeast, which makes the fungal enzyme a primary target for azole antimycotic drugs, while human and plant isoforms are potential targets for cholesterol-lowering drugs and herbicides (*14−16*). Different azole drugs widely used for treatment of fungal infections are also reported to be effective against lower eukaryota from the family Trypanosomatidae (order Kinetoplastida) (*17−23*). All organisms in this family are obligate parasites, often highly pathogenic, causing deadly diseases in human and cattle. (*24*). At present, the health of about a half a billion people is threatened with sleeping sickness (*Trypanosoma brucei* (TB) *gambiense* and TB *rodesiense*), Chagas disease (*T. cruzi*), and different types of leishmaniasis. Even 100 years after discovery of the source of these

infections, no drugs or vaccines are available that can ensure cures. Medications used currently are highly toxic, not very specific, and effective predominantly during the early stages (*25*). Antifungal azoles are known to increase survival of infected animals, inhibit growth of cultured forms of the parasites, and change sterol composition in kinetoplastid cells causing sharp increase in the concentration of the three substrates of 14α-DM: LS, MDL, and obtusifoliol (*26−30*).

BLAST search in the databases of emerging Trypanosomatidae genomes reveals four CYP51 sequences (*T. brucei, T. vivax, T. cruzi*, and *Leishmania major*) (Figure 1). The sequences share 74−86% amino acid identity and show strongest homology to CYP51 from *Mycobacterium tuberculosis* (MT) (28%), tomato (28%), and human (27%). On average, their identity to the rest of the CYP51 family is 25%, similar to that of CYP51 isoforms across kingdoms (*22−33*) (*31*). The sequences contain most of the regions of P450 and CYP51 family conservation (*5*), including a motif −YxxxxxPxFGxxV− in the B′-helix (*32*) and the

−HTS− triad in the I-helix (*33*). However, several of the amino acids conserved throughout the rest of the CYP51 family, which in the structure of MTCYP51 (1e9x) are located within the substrate binding cavity (B′C-loop and helices F and G) and found to be essential for the interaction with LS and DHL (*32*), are different in all the protozoan sequences.

We have cloned, expressed, and purified CYP51 from *T. brucei* and characterized it in comparison with CYP51 isoforms from other biological kingdoms. The protozoan P450 demonstrates altered affinity in comparison with human CYP51 toward three tested azole inhibitors (the highest, K_d = 0.45 μM, being detected with fluconazole) and reveals obvious substrate preference toward obtusifoliol. We hypothesize that obtusifoliol specificity of TBCYP51 reflects a novel, linear sequence of the reactions in the sterol biosynthesis in kinetoplastids (squalene 2,3-epoxide → LS→ MDL→ obtusifoliol).

EXPERIMENTAL PROCEDURES

Identification of Putative CYP51 Sequences in Trypanosomatidae. Sequence data for the genomes of *T. cruzi*, *T. vivax*, and *L. major* were obtained from the websites of The Institute of Genomic Research (http://www.tigr.org) and Sanger Center (http://www.sanger.ac.uk). A tblastn homology search was made using as a template the protein sequence of lanosterol 14α-DM from *T. brucei brucei* (NCBA accession number AAP33132). Alignment of 45 CYP51 proteins with four new protozoan sequences was performed by Clustal W1.81, analyzed in GeneDoc (2.6), and prepared in ESPript 2.1 programs with human and MTCYP51 sequences shown in Figure 1.

Cloning of CYP51 and CPR from T. brucei. The genes of CYP51 and CPR were PCR amplified from *T. brucei brucei* genomic DNA using the FailSafe PCR Premix Selection Kit (Epicenter). In the case of CYP51, the upstream primer 5′-CGC<u>CATATG</u>**GCT**CTTGAAGTTGCC-3′ corresponding to the TBCYP51 cDNA from 3 to 14 bp contained a unique *Nde*I cloning site (underlined) and modification of the second codon to alanine (**bold**) to optimize expression in *Escherichia coli* cells (*34*). The downstream primer 5′-CGC<u>AAGCT-T</u>**CTA**<i>GTGATGGTGATG</i>AGCAGCTGCCGCCTTCC-3′ incorporated a unique *Hin*dIII cloning site (underlined) followed by a stop codon (**bold**) and C-terminal 4-histidine tag (*italic*) and was complementary to TBCYP51 sequence from 1443 to 1426 bp. For CPR, the upstream 5′-CGC<u>CATATG</u>-GAGACCAAAGCAATAATGC-3′ and downstream 5′-CG-C<u>AAGCTT</u>**CTA**<i>GTGATGGTGATG</i>CGCCGTC-CAGACATCC-3′ primers were of similar construction. The PCR reaction included 50 ng of genomic DNA, 1 μM each forward and reverse primers, 0.5 μL of FailSafe PCR Enzyme in a final volume of 25 μL; 25 μL of FailSafe PCR 2× Premix D was added, and amplification was carried out by denaturation at 95 °C for 2 min, then 28 cycles of denaturation at 95 °C for 60 s, annealing at 52 °C for 30 s, and extension at 72 °C for 140 s. A terminal extension for 2 min at 72 °C completed the reaction. The PCR products from four separate reactions were purified from an agarose gel and subcloned into pGEM-T Easy vector (Promega). The correctness of the inserts was confirmed by DNA sequencing. Upon cloning, one difference from the sequence of TB-

CYP51 deposited into the NCBA database, valine instead of glutamic acid at position 107 (A320T in the cDNA), was found in all the samples (Figure 1). The residue has not been mutated to glutamic acid because valine is present in this position in all plant and two protozoan sequences, while the other CYP51 isoforms (*32*) including *T. cruzi* have threonine here and none contains glutamic acid. Site-directed mutagenesis was carried out using the QuickChange mutagenesis kit (Stratagene). The insert was excised by digestion with *Nde*I (New England Biolabs) and *Hin*dIII and cloned into the pCW expression vector (*34*). Because of two internal *Hin*dIII sites, the insert of TBCPR was digested from pGEM-T with *Nde*I/ *Sal*I and cloned into pCW using the same sites. The expression plasmids were sequenced again and transformed into *E. coli* HMS-174 cells (Novagen).

Protein Expression and Purification. CYP51 from MT, human, and *Candida albicans,* rat CPR, *E. coli* flavodoxin and flavodoxin reductase (Fld/FdR), and bovine adrenodoxin and adrenodoxin reductase (Adx/AdR) were expressed and purified as described previously (*35−38*). TBCYP51 was expressed at the conditions similar to the human isoform (*32*) with several modifications as follows. After induction with 0.5 mM IPTG followed by addition of δ-aminolevulinic acid to 0.5 mM concentration, *E. coli* cells were grown at 27 °C and 180 rpm for 44 h, harvested, resuspended in 100 mM Tris-acetate, pH 8.0, containing 500 mM sucrose and 0.5 mM EDTA, and incubated on ice for 20 min with 0.5 mg/ mL lysozyme. Then 0.5 mM PMSF was added, and the cells were pelleted by centrifugation and frozen at −70 °C. The pellet from 3 L of culture was resuspended in 50 mM Tris-HCl, pH 7.6, containing 1 mM EDTA, 10% glycerol, 100 mM NaCl, 0.2% Triton X-100, 1 mM DTT, and 0.5 mM PMSF, sonicated with a Branson sonifier, and ultracentrifuged at 100000g for 30 min to remove insoluble material. TBCYP51 was purified in two chromatographic stages, including Ni-chelating affinity column as described for human CYP51 (*32*) and Q-Sepharose (Pharmacia) equilibrated with 50 mM potassium phosphate buffer, pH 7.6, containing 0.5 mM EDTA, 10% glycerol (buffer A), and 0.1 mM phenylmethanesulfonyl fluoride (PMSF). After washing with equilibration buffer, TBCYP51 was eluted with linear gradient of NaCl (100−400 mM), concentrated up to ∼0.2 mM, and stored at −70 °C. TBCPR was expressed and purified by combination of Ni-chelating affinity column and chromatography on ADP−Sepharose (*36*). Molecular weight and purity of the proteins were confirmed by 12% SDS−PAGE.

Spectral Characterization. Spectra were taken at room temperature in buffer A containing 100 mM NaCl (buffer B) using a Beckman DU 640 spectrophotometer. Spin state of the ferric P450 was estimated from the ratio $\Delta A_{393−470}/ \Delta A_{417−470}$, assuming that values of 0.4 and 2.2 correspond to 0% and 100% high-spin form, respectively (*38*). The $Na_2S_2O_4$-reduced carbon monoxide complex (CO) difference spectra were used to measure precise P450 concentration (*39*) and to confirm absence of conversion into the inactive P420 form. Ligand-induced spectral changes were monitored as difference type I and type II spectral responses. Highly hydrophobic sterols (LS, DHL, 24-MDL, and obtusifoliol) were added from 0.5 mM stock solution in 45% 2-hydroxypropyl-β-cyclodextrin (HPCD) (Cyclodextrin Technologies Development, Inc). Imidazole, ketoconazole, and flu-

conazole (ICN Biomedicals, Inc) were dissolved in DMSO. For each titration, three binding assays of eight ligand concentrations in the range of $1-20$ μM for sterols and $1-60$ μM ($10-500$ μM in case of low affinity) for the azole inhibitors were performed. Apparent dissociation constants and maximal spectral response per nanomole of P450 were determined as previously described (*32*).

Electron Donor System. The capacity of the cloned TBCPR, rat microsomal CPR, mitochondrial Adx/AdR, and water-soluble *E. coli* Fld/FdR to reduce TBCYP51 was determined by formation of the CO-complexes (*32*). Before reduction, the concentrated CYP51 was incubated with potential electron donors at molar ratios 1:2 for TB and rat CPR, 1:4:1 for Adx/AdR, and 1:20:2 for Fld/FdR for 10 min at 24 °C. The efficiency of enzymatic reduction was calculated as percentage of P450−CO complex determined in the samples upon reduction with sodium hydrosulfite: $\Delta A_{450-490}(\text{NADPH})/\Delta A_{450-490}(\text{Na}_2\text{S}_2\text{O}_4)$ (%).

Enzyme Assays. LS, DHL, MDL, and obtusifoliol were isolated from plant and fungal sources (*40, 41*). MDL and obtusifoliol were labeled with ^{3}H at positions 28 and 3, respectively (*42, 43*). [3-^{3}H]LS was from American Radio-labeled Chemicals, Inc. For reconstitution of the CYP51 enzymatic activity unlabeled and [^{3}H]-sterols were mixed to give ~2000 cpm/nmol. Two different mixtures of 0.5 mM sterols were utilized to reconstitute catalytic activity of TBCYP51. In 10× substrate mixture 1, 10 mg/mL Tween 80 was used to disperse the sterols (*32*), while 10× substrate mixture 2 contained sterols dissolved in 45% HPCD. Composition of the rest of the reaction mixture was the same as that described for human CYP51 (*32*). Because of low solubility of the sterols and low affinity of TBCYP51 toward LS and MDL, we varied the concentration of P450 in the reaction from 1 to 10 μM at constant concentration of the sterols (50 μM) and P450/CPR ratio 1:2 (M/M). The identity of the CYP51 metabolites was confirmed by GC−MS using Hewlett-Packard 5973 gas chromatograph−mass spectrometer (capillary temperature 240 °C, vaporizer temperature 350 °C, flow rate of the carrier gas (He) 1.0 mL/min). Activities of other CYP51 isoforms were determined at the same conditions using rat CPR as an electron donor for human and *C. albicans* CYP51 and the *E. coli* electron donor system (P450/Fld/Fdr = 1:20:2 (M/M)) to support activity of MTCYP51.

RESULTS

Cloning, Expression and Purification of TBCYP51. Because the protein from TB is a microsomal P450 (in contrast to the soluble MTCYP51, it has a 24 amino acid hydrophobic N-terminal signal anchor sequence (*4*)), the pCW vector successfully used in expressing many microsomal P450s (*34*) was chosen for expression. TBCYP51 is expressed in *E. coli* at $450-500$ nmol of P450 per liter of culture. Two-step purification results in about 40% yield (~200 nmol/L) of electrophoretically pure protein (Figure 2, lane 3) with specific heme content of 17.5 nmol/mg. Purified TBCYP51 revealed a typical absolute absorbance spectrum of oxidized P450 (Figure 3A) with Soret maximum at 417 nm (calculated molar absorption ϵ_{417} = 117 mM^{-1} cm^{-1}), α- and β-bands at 568 nm (ϵ = 11.1 mM^{-1} cm^{-1}) and 536 nm (ϵ = 12.8 mM^{-1} cm^{-1}), and a spectrophotometric index of OD$_{417}$/OD$_{278}$
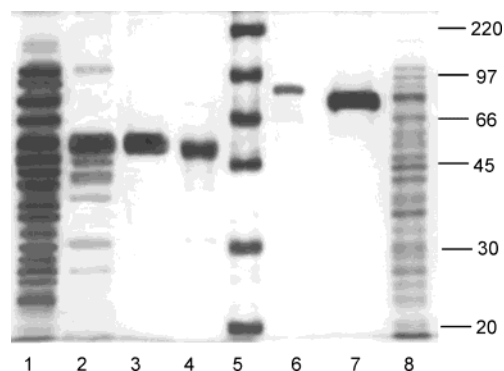
FIGURE 2: Expression and purification of TBCYP51 and TBCPR analyzed using 12% SDS−PAGE: lanes 1−3, TBCYP51 (481 amino acids, MW 54 kDa), expression in *E. coli* cells, eluate from Ni-column, and eluate from Q-column, respectively; lane 4, MTCYP51 (50 kDa); lane 5, Rainbow marker (Amersham Biosciences); lane 6, rat CPR (MW 80 kDa); lanes 7 and 8, TBCPR (635 amino acids, MW 71 kDa), purified sample and expression in *E. coli* cells, respectively.

= 1.8. At 24 °C in the absence of substrate, it contained about 95% of the low-spin form ($\Delta A_{393-470}/\Delta A_{417-470}$ = 0.49). The charge-transfer band at 648 nm also implies the presence of some high-spin form in the sample. The reduced CO spectrum (Figure 3B) has a maximum at 447 nm and is quite stable at room temperature in the absence of detergent. P420 content does not exceed 5%.

Figure 3C,D shows ligand binding spectra obtained upon titration of TBCYP51 with obtusifoliol and fluconazole. The type I difference spectrum induced by obtusifoliol is typical for P450s, and the spectral response to azole binding (type II spectral response) is slightly altered in shape, containing a trough with a plateau between 407 and 390 nm. Such a shape is sometimes seen in difference spectra of other azole-bound P450s and might reflect a combination of type II and reverse type I spectra (*4*) because interaction of the azole nitrogen with the heme iron causes transition of the five-coordinated high-spin portion of P450 into a six-coordinated low-spin form.

Interaction with Sterols. Contrary to azole binding, functional interaction of P450 with substrate leads to spin-state transition of the iron from a six-coordinated low- to a five-coordinated high-spin form. The transition results in blue shift of the Soret maximum (from 417 to 394 nm) and occurs because of displacement of a water molecule from the binding site (*44*). Type I spectral response to sterol binding was used to compare the affinity of TB and human CYP51 toward four known natural substrates of sterol 14α-DM (Table 1).

The results of titration of the human isoform are consistent with the observation that sterol 14α-demethylases from animals and fungi are able to bind and metabolize all four known CYP51 substrates equally well (*45*). In contrast, TBCYP51 under the same experimental conditions reveals clear type I spectral response only upon addition of obtusifoliol (K_d = 1.2 μM) (quite comparable values, K_d = 5.2 μM, ΔA_{max} per nanomole of P450 = 0.078, 24% increase in the high-spin content, were obtained upon titration of TBCYP51 with an artificial ligand 24(28)-dihydroobtusifoliol (data not shown)). The dissociation constants calculated for the three other substrates of CYP51 are above the maximal concentration of the added sterols (20 μM) and thus probably
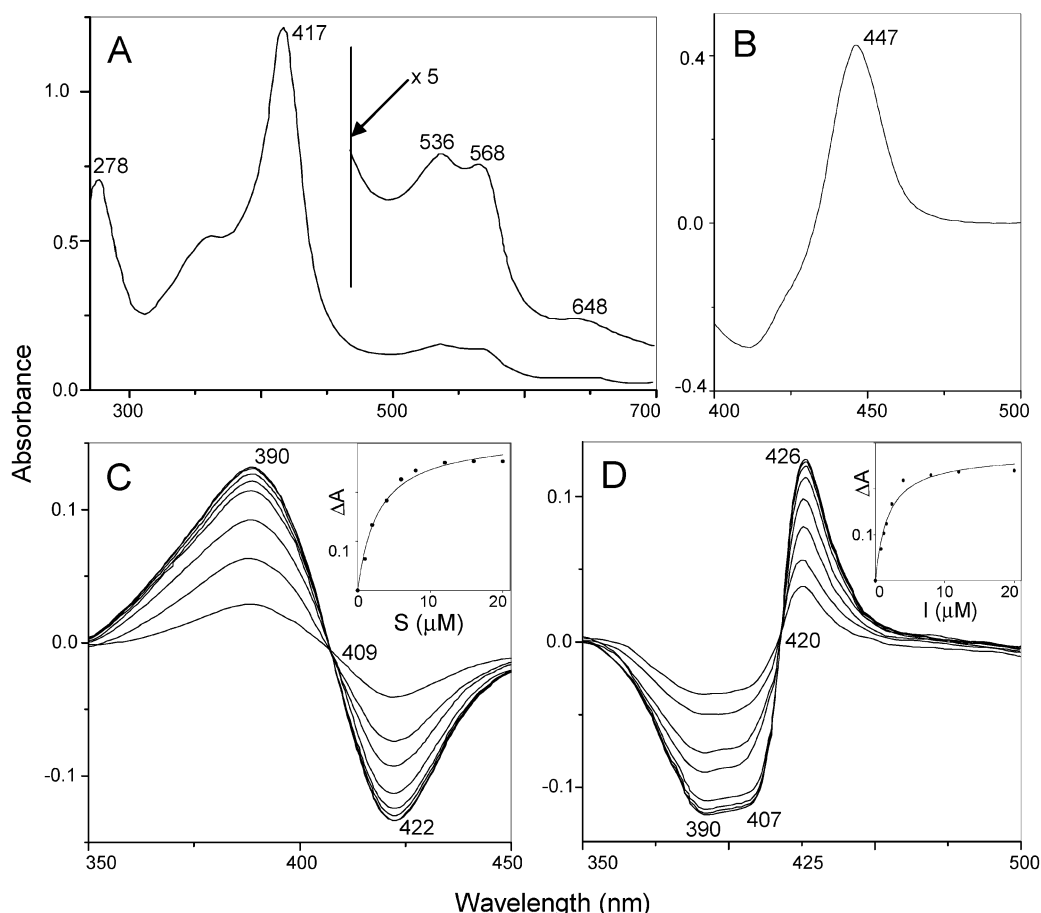
FIGURE 3: Optical absorbance of purified TBCYP51: (A) UV−visible absolute spectrum of oxidized form; (B) reduced carbon monoxide difference spectrum; (C) type I spectral response to obtusifoliol, 0.5−20 μM (substrate binding) (inset, titration curve, $\Delta A = \Delta A_{390-420}$); (D) type II spectral response to fluconazole, 0.5−60 μM (inhibitor binding) (inset, titration curve, $\Delta A = \Delta A_{426-407}$). The spectra were recorded at P450 concentrations 10.1, 4.7, 3.3, and 4.5 μM, respectively. Wavelength maxima, troughs, and isosbestic points are indicated.

Table 1: Type I Spectral Response of TB and Human CYP51 to Sterol Binding[a]

compound tested	TBCYP51			human CYP51		
	K_d, μM	ΔA_{max}/nmol[b]	Δhs, %[c]	K_d, μM	ΔA_{max}/nmol	Δhs, %
LS[d]	97 ± 15	0.011 ± 0.005	e	0.5 ± 0.02	0.047 ± 0.001	25
DHL	84 ± 14	0.011 ± 0.003	e	0.5 ± 0.03	0.048 ± 0.001	25
MDL	24 ± 3.1	0.027 ± 0.003	8	2.4 ± 0.2	0.059 ± 0.001	24
obtusifoliol	1.2 ± 0.1	0.093 ± 0.001	48	1.4 ± 0.19	0.041 ± 0.002	19

[a] Results are presented as a mean $\pm$ standard deviation. [b] Optical units. [c] Increase in the percentage of high-spin content calculated from absolute absorbance spectra after titration. [d] See Figure 7 and Supporting Information. [e] Not detected.

not precise, especially in the case of LS and DHL. Absolute absorbance spectra after the titration with these two sterols do not show any increase in percentage of high-spin content, and the calculated maximal amplitude of the difference spectra does not exceed 10% per nanomole of P450 (0.12 ou/nmol is taken as 100%). Thus, the angular (4β-) methyl group (obtusifoliol → MDL) decreases the affinity of TBCYP51 toward sterols by more than 1 order of magnitude, and reduction of the volume of the sterol side chain at position 24 (MDL → DHL) or flattening of the nucleus by the additional dehydrogenation (DHL → LS) adds one more order of magnitude to the decrease. The observed differences between the affinities of the two CYPs toward the tested sterols suggest that, in contrast to the human isoform, only obtusifoliol can be the relevant substrate of TBCYP51.

Enzymatic Reduction of TBCYP51. Lack of the ability of TBCYP51 to efficiently accept electrons from yeast CPR

was one of the proposed explanations for modest changes in the LS/ergosterol ratio detected in vivo in an *erg11*-deleted *Saccharomyces cerevisiae* strain complemented with an expression vector carrying the TBCYP51 gene (*46*). Therefore, we cloned endogenous CPR from TB genomic DNA; the sequence corresponds to that deposited into the NCBA database (accession number AAP37031) with the exception that it contains a GGA codon (glycine 243) instead of AGA (arginine 243). The glycine codon is also found in the preliminary sequence of TBCPR from the Sanger Center database. The protein was expressed in *E. coli* cells, was purified to electrophoretic homogeneity (Figure 2, lane 7) with a yield of about 120−140 nmol/L culture, had spectrophotometric indices $OD_{280}/OD_{456} = 7.4$ and $OD_{456}/OD_{380} = 1.1$ (data not shown), and was able to reduce human CYP51 with 65% efficiency of chemical reduction with $Na_2S_2O_4$ (Figure 4). Efficiency of TBCPR as electron donor
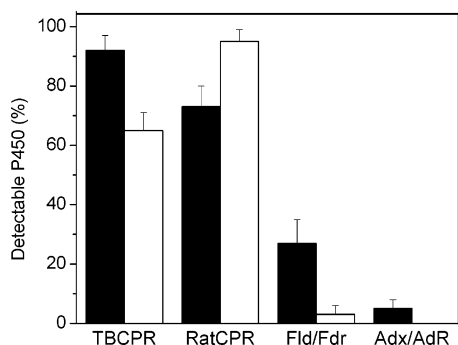
FIGURE 4: Enzymatic reduction. Efficiency of reduction of TB-CYP51 (black columns) with NADPH through endogenous TBCPR and three exogenous electron donor systems, rat CPR, *E. coli* Fld/Fdr, and bovine Adx/AdR, in comparison to the reduction of human isoform (white columns) is presented. Data of two independent experiments are summarized; the differences between the two values are shown with the bars. 100% indicates chemical reduction by $Na_2S_2O_4$.

to its endogenous partner TBCPR is about 90%. Regardless of low sequence identity between TB and rat CPR (35%), the ability of TBCYP51 to accept electrons through rat CPR is also quite high (~73%), which is not surprising because in vivo CPR is usually not very specific and supports activities of a large number of microsomal CYPs from different families (*4*). Other systems known to reduce eukaryotic P450s, water-soluble *E. coli* Fld/FdR and mitochondrial Adx/AdR electron donor systems demonstrated 27% and 5% efficiency of TBCYP51 reduction, respectively, and no P450 reduction was observed with NADPH alone. Thus, TBCYP51 prefers its endogenous microsomal electron donor system, but the effective reduction with rat CPR suggests that the lack of the homologous electron donor in the yeast system mentioned above is not the reason for modest LS conversion. Rather it is the substrate preference of TBCYP51.

Reconstitution of Enzymatic Activity of TBCYP51. At 10 μM P450, sterol 14α-demethylation of obtusifoliol is practically complete within 5 min (Figure 5A). Under the same conditions, conversion of MDL and LS occurs much more slowly. Two polar peaks identified by GC-MS as a mixture of the CYP51 reaction intermediates 14α-hydroxymethyl and 14α-carboxyaldehyde at the ratio ~1:3 appear first. Upon conversion of MDL (Figure 5B), the percentage of the intermediates in the reaction decreases in time, and after 4 h of incubation, the HPLC profile shows predominantly 14α-demethylated product. In contrast, when LS is used as a substrate (Figure 5C), after 4 h of incubation, the intermediates still dominate in the reaction and the HPLC profile does not change, though CO spectra indicate that more than 40% of the initial amount of TBCYP51 remains in the P450 form (not shown). Calculated at these conditions, maximal rates of LS and MDL 14α-demethylation are 0.009 and 0.015 nmol of product per nanomole of P450 per minute, respectively. Under the same conditions no conversion of two obtusifoliol derivatives (14α-methy-24(28)-methylenecholest-8-en-3β-ol and 14α-methyl-24(28)-methylenecholest-9-en-3β-ol) (Supporting Information) lacking both methyl groups at C4 and hypothesized as potential substrates for Trypanosomatidae sterol 14α-DM (*28*) was observed.

If the reaction is carried out at 1 μM P450, conversion of LS and MDL stops at the stage of the intermediates (Table

2). Under the same conditions, obtusifoliol is predominantly metabolized to the product, giving a maximal calculated turnover number of 5.6 nmol/((nmol of P450)·min). Using rat CPR as an electron donor for TBCYP51 decreases the rate of sterol conversion by 50% but does not affect substrate preference of the enzyme. In substrate mixture 1 (sterol/detergent), generally used for reconstitution of sterol 14α-DM activity (*32, 47−49*), TBCYP51 does not show any LS or MDL metabolism. The rate of obtusifoliol conversion in the absence of HPCD also decreases. HPCD is widely used in pharmacology and protein chemistry to increase solubility of a variety of lipophilic compounds, to ensure their delivery in vivo to hydrophobic binding sites (membranes), and also to stabilize and even refold proteins (*50, 51*). It was found that dissolving cholesterol in HPCD increases activity of CYP11A1 (*52*). Our results suggest that HPCD helps to deliver hydrophobic sterols to the substrate-binding pocket of TBCYP51, but because of the lack of affinity of this CYP51 isoform to LS (MDL), the majority of the sterol molecules are not bound properly to undergo all three stages of the CYP51 catalytic cycle. This suggestion is in good agreement with the absence of spin steps changes of TBCYP51 heme iron upon addition of LS/DHL (or very modest increase in the high-spin content in response to MDL) and is supported by the finding that conversion of LS stops after formation of the intermediates with the 14α-demethylated product appearing only at 10-fold increased concentration of P450.

In contrast to TBCYP51, human, *C. albicans*, or MT isoforms at the same experimental conditions metabolize each of the three tested sterols with very similar rates (Figure 6). Without influencing substrate specificity, HPCD increases the tendency of all three CYP51s to produce intermediates (up to about 10−15% of the amount of the product of the reaction (not shown)) and leads to at least 2-fold faster turnover of microsomal but not soluble MTCYP51. The rate of obtusifoliol conversion by TBCYP51 in the presence of HPCD (substrate mixture 2) is of the same order as turnover by human and *C. albicans* isoforms, 600-fold higher than its ability to 14α-demethylate LS and 300-fold faster than 14α-demethylation of MDL. Thus obtusifoliol is very likely to be the physiological substrate for TBCYP51.

Interaction with Azole Inhibitors. Ketoconazole and fluconazole are well-known sterol 14α-DM inhibitors, commercial antifungal agents widely used for treatment of different kinds of mycoses (*14−16*). While affinity of TBCYP51 toward ketoconazole (where the coordination nitrogen comes from an imidazole group) is quite moderate (K_d = 4.4 μM) and 40-fold lower than that of the human isoform (K_d = 0.11 μM), its binding to the triazole nitrogen of fluconazole is 1 order of magnitude tighter (K_d = 0.37 μM) (Table 3). Interestingly, human sterol 14α-DM in the same range of concentrations weakly interacts with fluconazole, the type II spectral response being detected only above 10 μM. Imidazole usually does not bind tightly to P450s; binding of this relatively small molecule lacks van der Waals interactions with remote hydrophobic regions of the hemoprotein substrate-binding pocket (*13*). The affinity of TB-CYP51 toward imidazole is also quite low (K_d = 21 μM) but about 10-fold higher than that determined for human ortholog. Together, these data imply that ligand binding of the two isoforms of 14α-DM (from host and parasite) differ
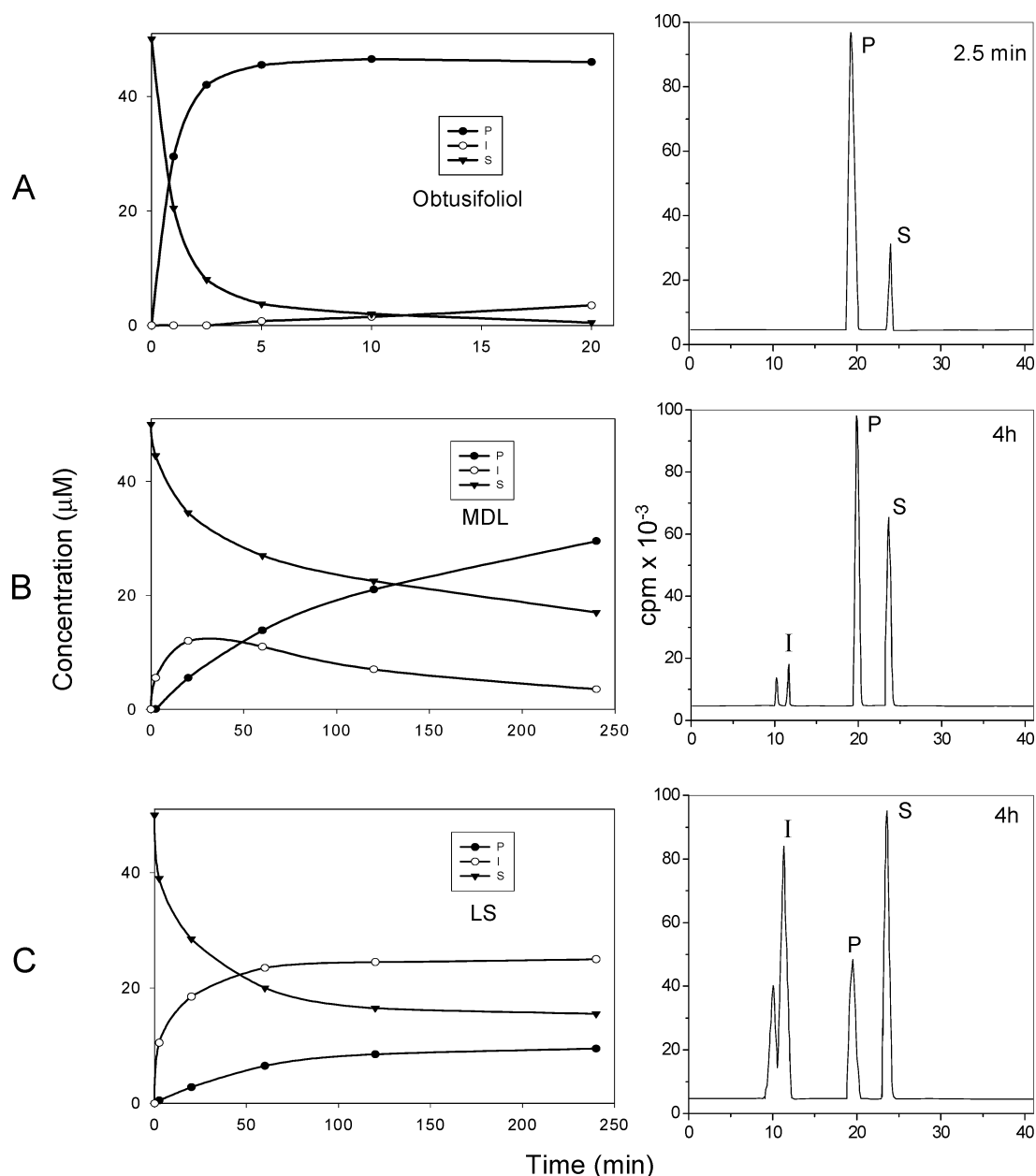
FIGURE 5: Catalytic activity of TBCYP51 for 14α-demethylation of obtusifoliol (A), MDL (B), and LS (C). Final concentration of P450 in the reaction mixture is 10 μM. The right column presents reverse-phase HPLC profiles of radiolabeled metabolites formed in the reconstituted system after incubation with obtusifoliol (2.5 min), MDL, and LS (4 h). The peaks at 19−20 (P) and 22−23 (S) min correspond to the product and substrate retention times, respectively. The peaks at 9−12 min (I) correspond to the CYP51 intermediates, an alcohol (9−10 min) and an aldehyde (11−12 min). The left column presents the time course of the sterol 14α-DM reaction for the concentration of the product (●), the intermediates (○), and the substrate (▼). Data represent the average result of four measurements for each substrate.

Table 2: Rates of Conversion of Obtusifoliol, MDL, and LS by TBCYP51 (1 μM)

| | turnover number, nmol/((nmol of P450)·min) | | | |
| | sterol/Tween 80[a] | | sterol/HPCD | |
substrate	product	intermediate	product	intermediate
obtusifoliol	0.63 ± 0.02	0.022 ± 0.005	5.6 ± 0.2	0.38 ± 0.05
MDL	0	0	0	0.22 ± 0.01
LS	0	0	0	0.71 ± 0.06

[a] Sterols (50 μM final) were added from 10× substrate mixture 1 (sterol/Tween 80) or 10× substrate mixture 2 (sterol/HPCD) as described in Experimental Procedures. Duplicate determinations of four separate experiments were performed; the data are expressed as mean ± standard deviation.

not only in terms of their substrate specificity but also in preferences toward inhibitors. In vitro screening of azole compounds is quite promising for selection and further design of inhibitors highly specific toward the parasitic isoform of CYP51, and testing of a larger panel of azole derivatives and artificial substrate analogues is underway.
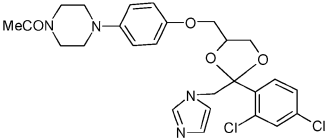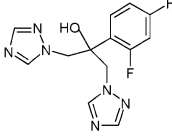
DISCUSSION

The profound specificity of TBCYP51 toward obtusifoliol must be connected with the topology of the substrate-binding cavity, which in the linear sequence of P450s is mostly represented by the six substrate recognition sites (SRS) (*53*) (Figure 1). Our previous studies of MTCYP51 structure (*32*), suggested that low affinity of the protozoan isoforms of CYP51 toward LS might be caused by substitutions of the conserved amino acids within SRSs 1, 2, and 3, mutation of which completely abolishes the ability of MTCYP51 to bind LS and DHL. On the basis of these findings, we originally

Table 3: Interaction of TB and Human CYP51 with Azole Inhibitors[a]

| CYP51 | type II spectral response | | | | | |
| | imidazole | | ketoconazole | | fluconazole | |
	Kd, μM	ΔA_{max}/nmol	Kd, μM	ΔA_{max}/nmol	Kd, μM	ΔA_{max}/nmol
TB	21.4±1.7	0.064±0.002	4.4±0.5	0.08±0.001	0.37±0.06	0.056±0.003
human	189±13	0.071±0.003	0.11±0.01	0.07±0.002	40.2±3.4	0.053±0.001

[a] The results of four titration experiments are summarized and presented as a mean ± standard deviation.
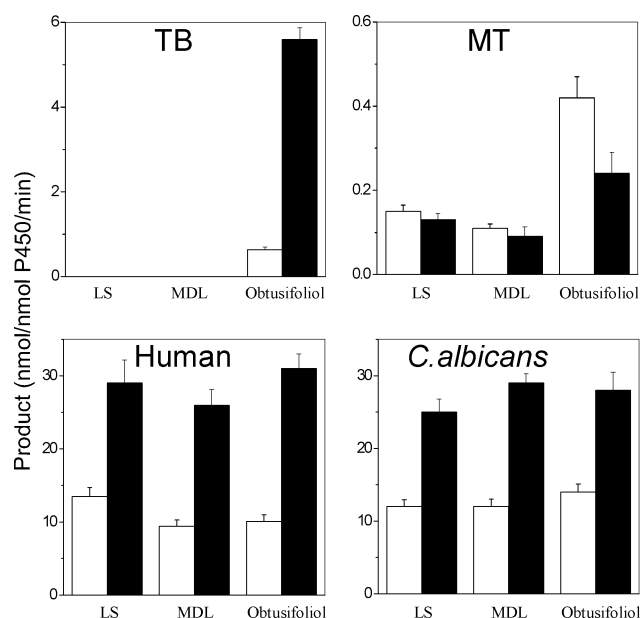
FIGURE 6: Turnover of CYP51 from different species. The reactions were carried out at 1 μM P450 in substrate mixture 1 (white columns) and 2 (black columns) as described in Experimental Procedures. Duplicate determinations of two separate experiments were performed, the data being expressed as mean ± standard deviation.

predicted that the protein deposited into the NCBA database as "lanosterol 14α-demethylase" might be unable to function as a 14α-DM. Conversion of the protozoan CYP51 gene into a pseudogene would support the hypothesis that Trypanosomatidae do not synthesize endogenous sterols using host cholesterol for the membranes (54). Mutagenesis of the five residues of TBCYP51, which align with D90, L172, G175, R194, and D195 in MTCYP51 to the amino acids conserved throughout about 50 other known isoforms of CYP51 (A117D, M204L, S207G, C229R, and H230D) did not, however, increase LS-metabolizing activity of either the single mutants or the mutant containing all five substitutions. In all cases, the 14α-carboxyaldehyde derivative was the main product in the HPLC profiles (Supporting Information). We connect absence of a positive effect of mutagenesis on the ability of TBCYP51 to metabolize LS with overall low sequence homology, particularly in the regions of SRS 2 and 3, between the four protozoan proteins and the rest of the CYP51 family.

Since high preference toward obtusifoliol is typical for plant sterol 14α-DM, the obtusifoliol specificity of TBCYP51 (regardless of the absence of any greater resemblance of the protozoan enzyme with plant isoforms) could indicate similarity of sterol biosynthesis in Trypanosomatidae with the plant pathway, especially taking into consideration that several matches to the plant metabolic processes have been demonstrated in the parasites (55). However, presence in all the sequenced protozoan genomes of LS synthase but not cycloarthenol synthase, experimental data showing that antifungal inhibitors of LS synthase cause sharp reduction in lanosterol and ergosterol in the cultured parasites (56), and no traces of cycloartenol in the cells point out that, similarly to the fungi/animals pathway, the sequence of the reactions following squalene 2,3-epoxide cyclization in Trypanosomatidae starts from LS (Figure 7).

On the other hand, the profound preference of TBCYP51 toward obtusifoliol in contrast to the five other compounds tested in this study clearly shows that the 24-methyl group and equatorial methyl group at position 4 are both required for a 14α-methyl sterol to be a substrate for the protozoan CYP51. This indicates that in the subsequent part of the pathway both 24-methylation and elimination of the 4β-methyl group of LS must precede 14α-demethylation. Conversion of LS into obtusifoliol can occur either through MDL or through 4α,14α-dimethylcholesta-8,24-dien-3β-ol. The possibility that 4-demethylation takes place as a first step, before 24-methylation, is lower because the traces of 4α,14α-dimethylcholesta-8,24-dien-3β-ol, as well as 14α-methylcholesta-8,24-dien-3β-ol, have only been observed in cultured Trypanosomatidae cells upon treatment with aza-sterols (inhibitors of sterol methyltransferase) (57). In contrast, LS, MDL, and obtusifoliol are always found in kinetoplastids, sharply increasing in concentration upon inhibition with azole derivatives (26, 29, 30.). Thus, under normal physiological conditions, the pathway LS → MDL → obtusifoliol must be kinetically favored in Trypanosomatidae. This difference from the fungal pathway where the CYP51 reaction occurs both before (LS) and after side chain methylation (MDL) but always precedes elimination of a methyl group at position 4 explains the low ability of TBCYP51 to metabolize LS in vivo in the *erg11*-deficient yeast strain where obtusifoliol is not formed (46).
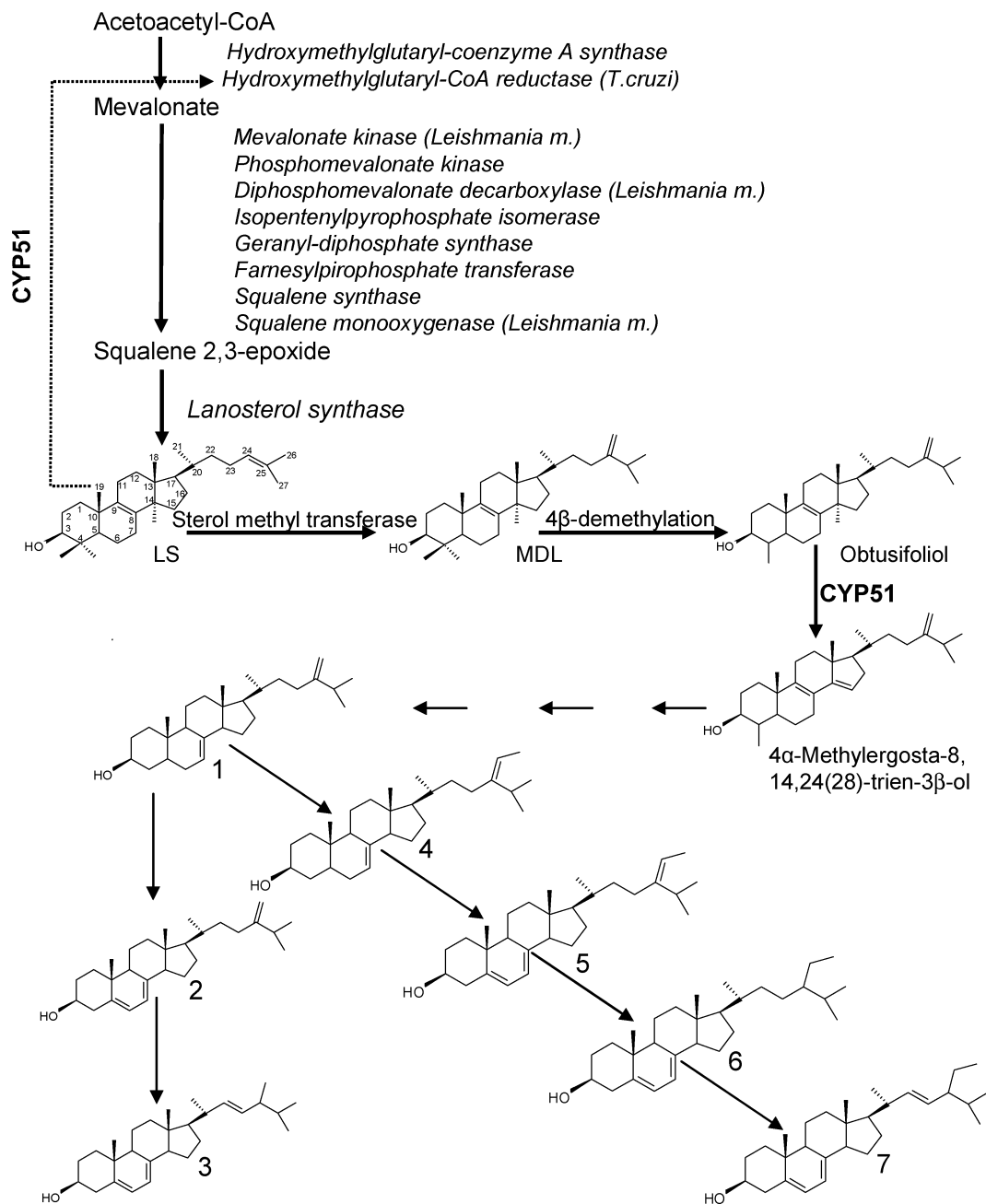
FIGURE 7: Suggested sterol biosynthetic pathway in Trypanosomatidae. All the enzymes of the general for eukaryotic cells part of the pathway are found using BLAST search in the protozoan genomes, most taken from the genome of TB, otherwise being specified in brackets. Sterol 4-demethylation includes two enzymes, methylsterol monooxygenase (EC1.14.13.72) and 3β-hydroxy-4α-methylcholestenecarboxylate 3-dehydrogenase (EC 1.1.1.170), the sequences of which have not yet been found. Bold arrows show the most likely sequence of the reactions; the dotted arrow represents a hypothesized possibility. Compound designation are as follows: **1**, ergosta-7,24-(28)-dien-3β-ol (episterol); **2**, ergosta-5,7,24(28)-trien-3β-ol (5-dehydroepisterol); **3**, ergosta-5,7,22-trien-3β-ol (ergosterol); **4**, stigmasta-7,24(28)-dien-3β-ol (Δ7-sitosterol); **5**, stigmasta-5,7,24(28)-trien-3β-ol; **6**, stigmasta-5,7-dien-3β-ol (Δ5,7-sitosterol); **7**, stigmasta-5,7,22-trien-3β-ol.

Starting from episterol (**1**) part of the pathway in Figure 7 includes the compounds **1**−**7** found in the kinetoplastids at different stages of their life cycle, monoalkylated ergosterol (**3**) and double alkylated stigmasta-5,7,22-trien-3β-ol (**7**) being the most abundant products (25−40% and 15−30% of total content of intracellular sterols) (*26, 29, 30, 58, 59*). While ergosterol is the main product of fungal sterol biosynthesis, stigmasterols (**4**−**7**) are typical in plants (*2, 3*).

The exact role of 24-alkyl sterols in Trypanosomatidae is not clear. Yet, it is known that in *T. cruzi* and different species of *Leishmania* they cannot be replaced by exogenous

cholesterol (*60*). In general, the sterol composition determines membrane fluidity and permeability, modulating activity of membrane-bound enzymes. It has been supposed that in addition to this structural role in the membranes, similarly to plant phytohormones, 24-alkylated sterols in Trypanosomatidae might participate in cell development and regulation of their complicated life cycle shuttling between insect vectors and vertebral or plant hosts (*28*). In this connection, the unique sequence of the reactions LS → MDL → obtusifoliol might be either evolutionarily older than the pathways known in other eukaryota (Supporting Information) or could have developed in the parasites as an opportunity

for certain stages of the life cycle (e.g., exponentially dividing) to use host substrates for faster formation of particular final products regardless of what host (vertebrata or plant) they infect. Such a pathway, always going through obtusifoliol but able to include host 14α–methylsterols, would reflect adaptation of the parasites to survive in extremely different environments. If so, then the tendency of TBCYP51 to form the 14α-carboxyaldehyde derivative from LS detected in our reconstituted system in vitro (Figure 5C, Table 2) is not excluded to play a role in vivo. Similar to mammalian cells where it was found to modulate 3-hydroxy-3-methylglutaryl-CoA reductase activity upon cholesterol biosynthesis (*10−12*), in Trypanosomatidae the intermediate might down-regulate mevalonate production when an exogenous source of 14α-methyl sterols is available from the host.

Altogether, profound preference of TBCYP51 toward obtusifoliol indicates that the sterol biosynthetic pathway in Trypanosomatidae does not include several alternative branches (*28*, *60*) but is linear up to formation of 4α-methylergosta-8,14,24(28)-trien-3β-ol and includes sequential conversion: squalene 2,3-epoxide → LS → MDL → obtusifoliol. Specific inhibition of these stages of the pathway could be of great importance in developing a cure for sleeping sickness and other human diseases caused by the parasites.

ACKNOWLEDGMENT

SUPPORTING INFORMATION AVAILABLE

Scheme of biosynthesis of CYP51 substrates and sterol 14α-demethylation in eukaryotic kingdoms; structures of two 14α-methylsterols other than natural substrates of 14α-DM tested in the reconstituted reaction with TBCYP51 in this study; percentage of the substrate, intermediates, and the 14α-demethylated product in the HPLC profiles after the reaction of the mutant forms of TBCYP51 with LS. This material is available free of charge via the Internet at http://pubs.acs.org.

REFERENCES

1. Nes, W. R., and McKean, M. R. (1977) *Biochemistry of Steroids and Other Iisopentenoids*, pp 147−325, University Park Press, Baltimore.
2. Nes, W. R. (2000) Sterol methyl transferase: enzymology and inhibition, *Biochim. Biophys. Acta 1529*, 63−88.
3. Schaller, H. (2003) The role of sterols in plant growth and development, *Prog. Lipid Res. 42*, 163−175.
4. Omura, T., Ishimura, Y., and Fujii-Kuriyama, Y. (1993) *Cytochrome P450*, 2nd ed., Kodansha, Tokyo.
5. Yoshida, Y., Aoyama, Y., Noshiro, M., and Gotoh, O. (2000) Sterol 14-demethylase P450 (CYP51) provides a breakthrough for the discussion on the evolution of cytochrome P450 gene superfamily, *Biochem. Biophys. Res. Commun. 273*, 799−804.
6. Fischer, R. T., Trzaskos, J. M., Magolda, R. L., Ko, S. S., Brosz, C. S., and Larsen, B. (1991) Lanosterol 14 alpha-methyl demethylase. Isolation and characterization of the third metabolically generated oxidative demethylation intermediate, *J. Biol. Chem. 266*, 6124−6132.
7. Trzaskos, J. M., Fischer, R. T., and Favata, M. F. (1986) Mechanistic studies of lanosterol C-32 demethylation. Conditions which promote oxysterol intermediate accumulation during the demethylation process, *J. Biol. Chem. 261*, 16937−16942.
8. Shafiee, A., Trzaskos, J. M., Paik, Y. K., and Gaylor, J. L. (1986) Oxidative demethylation of lanosterol in cholesterol biosynthesis: accumulation of sterol intermediates, *J. Lipid Res. 1*, 1−10.
9. Aoyama, Y., Yoshida, Y., Sonoda, Y., and Sato, Y. (1987) Metabolism of 32-hydroxy-24,25-dihydrolanosterol by purified cytochrome P-45014DM from yeast. Evidence for contribution of the cytochrome to whole process of lanosterol 14 alpha-demethylation, *J. Biol. Chem. 262*, 1239−1243.
10. Tabacik, C., Aliau, S., Serrou, B., and Crastes de Paulet, A. (1981) Post-HMG CoA reductase regulation of cholesterol biosynthesis in normal human lymphocytes: lanosten-3 betal-ol-32-al, a natural inhibitor, *Biochem. Biophys. Res. Commun. 101*, 1087−1095.
11. Sonoda, Y., Obi, N., Onoda, M., Sakakibara, Y., and Sato, Y. (1992) Effects of 32-oxygenated lanosterol derivatives on 3-hydroxy-3-methylglutaryl coenzyme A reductase activity and cholesterol biosynthesis from 24, 25-dihydrolanosterol, *Chem. Pharm. Bull. (Tokyo) 10*, 2796−2799.
12. Trzaskos, J. M., Favata, M. F., Fischer, R. T., and Stam, S. H. (1987) In situ accumulation of 3 beta-hydroxylanost-8-en-32-aldehyde in hepatocyte cultures. A putative regulator of 3-hydroxy-3-methylglutaryl-coenzyme A reductase activity, *J. Biol. Chem. 262*, 12261−12268.
13. Ortiz de Montellano, P. R., and Correia, M. A. (1995) Inhibition of Cytochrome P450 Enzymes, in *Cytochrome P450: Structure, Mechanism, and Biochemistry*, 2nd ed. (Ortiz de Montellano, P. R., Ed.) pp 305−364, Plenum Publishing Corp., New York.
14. Marichal, P., Koymans, L., Willemsens, S., Bellens, D., Verhasselt, P., Luyten, W., Borgers, M., Ramaekers, F. C., Odds, F. C., and Bossche, H. V. (1999) Contribution of mutations in the cytochrome P450 14alpha-demethylase (Erg11p, Cyp51p) to azole resistance in *Candida albicans*, *Microbiology 145*, 2701−2713.
15. Asai, K., Tsuchimori, N., Okonogi, K., Perfect, J. R., Gotoh, O., and Yoshida, Y. (1999) Contribution of mutations in the cytochrome P450 14alpha-demethylase (Erg11p, Cyp51p) to azole resistance in *Candida albicans*, *Antimicrob. Agents Chemother. 43*, 1163−1169.
16. Favre, B., Didmon, M., and Ryder, N. S. (1999) Multiple amino acid substitutions in lanosterol 14alpha-demethylase contribute to azole resistance in *Candida albicans*, *Microbiology 145*, 2715−2725.
17. McCabe, R. E., Remington, J. S., and Araujo, F. G. (1986) In vitro and in vivo effects of itraconazole against *Trypanosoma cruzi*. *Am. J. Trop. Med. Hyg. 35*, 280−284.
18. Dogra, J., Aneja, N., Lal, B. B., and Mishra, S. N. (1990) Cutaneous leishmaniasis in India. Clinical experience with itraconazole (R51 211 Janssen), *Int. J. Dermatol. 9*, 661−662.
19. Vannier-Santos, M. A., Urbina, J. A., Martiny, A., Neves, A., and de Souza, W. (1995) Alterations induced by the antifungal compounds ketoconazole and terbinafine in *Leishmania*, *J. Eukaryotic Microbiol. 42*, 337−346.
20. Urbina, J. A., Payares, G., Molina, J., Sanoja, C., Liendo, A., Lazardi, K., Piras, M. M., Piras, R., Perez, N., Wincker, P., and Ryley, J. F. (1996) Cure of short- and long-term experimental Chagas' disease using D0870, *Science 273*, 969−971.
21. Kierszenbaum, F. (1996) Can a killer be arrested? *Nat. Med. 2*, 1071−1072.
22. Balana-Fouce, R., Reguera, R. M., Cubria, J. C., and Ordonez, D. (1998) The pharmacology of leishmaniasis, *Gen. Pharmacol. 30*, 435−443.
23. Buckner, F., Yokoyama, K., Lockman, J., Aikenhead, K., Ohkanda, J., Sadilek, M., Sebti, S., Van Voorhis, W., Hamilton, A., and Gelb, M. H. (2003) A class of sterol 14-demethylase inhibitors as anti-*Trypanosoma cruzi* agents, *Proc. Natl. Acad. Sci. U.S.A. 100*, 15149−15153.
24. Kreier, T., and Julius, P. (1991) *Parasitic Protozoa*, 2nd ed., Academic Press, San Diego, CA.
25. Hammarton, T. C., Mottram, J. C., and Doerig, C. (2003) The cell cycle of parasitic protozoa: potential for chemotherapeutic exploitation, *Prog. Cell Cycle Res. 5*, 91−101.
26. Goad, L. J., Berens, R. L., Marr, J. J., Beach, D. H., and Holz, G. G., Jr. (1989) The activity of ketoconazole and other azoles against *Trypanosoma cruzi*: biochemistry and chemotherapeutic action in vitro, *Mol. Biochem. Parasitol. 32*, 179−189.
27. Urbina, J. A. (2001) Specific treatment of Chagas disease: current status and new developments, *Curr. Opin. Infect. Dis. 6*, 733−741.
28. Roberts, C. W., McLeod, R., Rice, D. W., Ginger, M., Chance, M. L., and Goad, L. J. (2003) Fatty acid and sterol metabolism:

potential antimicrobial targets in apicomplexan and trypanosomatid parasitic protozoa, *Mol. Biochem. Parasitol. 126*, 129−142.

29. Urbina, J. A., Payares, G., Sanoja, C., Molina, J., Lira, R., Brener, Z., and Romanha, A. J. (2003) Parasitological cure of acute and chronic experimental Chagas disease using the long-acting experimental triazole TAK-187. Activity against drug-resistant *Trypanosoma cruzi* strains, *Int. J. Antimicrob. Agents 1*, 39−48.

30. Urbina, J. A., Payares, G., Sanoja, C., Lira, R., and Romanha, A. J. (2003) In vitro and in vivo activities of ravuconazole on *Trypanosoma cruzi*, the causative agent of Chagas disease, *Int. J. Antimicrob. Agents 1*, 27−38.

31. Lepesheva, G. I., and Waterman, M. R. (2004) CYP51- the omnipotent P450, *Mol. Cell. Endocrinol. 215*, 165−170.

32. Lepesheva, G. I., Virus, C., and Waterman, M. R. (2003) Conservation in the CYP51 family. Role of the B′ helix/BC loop and helices F and G in enzymatic function, *Biochemistry 42*, 9091−9101.

33. Nitahara, Y., Kishimoto, K., Yabusaki, Y., Gotoh, O., Yoshida, Y., Horiuchi, T., and Aoyama, Y. (2001) The amino acid residues affecting the activity and azole susceptibility of rat CYP51 (sterol 14-demethylase P450), *J. Biochem. (Tokyo) 129*, 761−768.

34. Barnes, H. J., Arlotto, M. P., and Waterman, M. R. (1991) Expression and enzymatic activity of recombinant cytochrome P450 17 alpha-hydroxylase in *Escherichia coli*, *Proc. Natl. Acad. Sci. U.S.A. 88*, 5597−5601.

35. Lepesheva, G. I., Podust, L. M., Bellamine, A., and Waterman, M. R. (2001) Folding requirements are different between sterol 14alpha-demethylase (CYP51) from *Mycobacterium tuberculosis* and human or fungal orthologs, *J. Biol. Chem. 276*, 28413−28420.

36. Shen, A. L., Porter, T. D., Wilson, T. E., and Kasper, C. B. (1989) Structural analysis of the FMN binding domain of NADPH-cytochrome P-450 oxidoreductase by site-directed mutagenesis, *J. Biol. Chem. 264*, 7584−7589.

37. Jenkins, C. M., and Waterman, M. R. (1998) NADPH-flavodoxin reductase and flavodoxin from *Escherichia coli*: characteristics as a soluble microsomal P450 reductase, *Biochemistry 37*, 6106−6111.

38. Usanov, S. A., Graham, S. E., Lepesheva, G. I., Azeva, T. N., Strushkevich, N. V., Gilep, A. A., Estabrook, R. W., and Peterson, J. A. (2002) Probing the interaction of bovine cytochrome P450scc (CYP11A1) with adrenodoxin: evaluating site-directed mutations by molecular modeling, *Biochemistry 41*, 8310−8320.

39. Omura, T., and Sato, R. (1964) Carbon monoxide-binding pigment of liver microsomes. II. Solubilization, purification, and properties, *J. Biol. Chem. 239*, 2379−2385.

40. Le, P. H., and Nes, W. D. (1990) Evidence for separate intermediate in the biosynthesis of multiple 24-*b*-methyl sterol end products by *Gibberella fujikuroi*, *Biochim. Biophys. Acta 1042*, 119−125.

41. Guo, D. A., Venkatramesh, M., and Nes, W. D. (1995) Developmental regulation of sterol biosynthesis in *Zea mays*, *Lipids 30*, 203−219.

42. Nes, W. D., Song, Z., Dennis, A. L., Zhou, W., Nam, J., and Miller, M. B. (2003) Biosynthesis of phytosterols. Kinetic mechanism for the enzymatic C-methylation of sterols, *J. Biol. Chem. 278*, 34505−34516.

43. Le, P. H., and Nes, W. D. (1986) Sterols: tritium labeling and selective oxidation, *Chem. Phys. Lipids 40*, 57−67.

44. Haines, D. C., Tomchick, D. R., Machius, M., and Peterson, J. A. (2001) Pivotal role of water in the mechanism of P450BM-3, *Biochemistry 40*, 13456−13465.

45. Lamb, D. C., Kelly, D. E., and Kelly, S. L. (1998) Molecular diversity of sterol 14-demethylase substrates in plants, fungi and humans, *FEBS Lett. 425*, 263−265.

46. Joubert, B. M., Nguyen, L. N., Matsuda, S. P., and Buckner, F. S. (2001) Cloning and functional characterization of a *Trypanosoma brucei* lanosterol 14alpha-demethylase gene, *Mol. Biochem. Parasitol. 117*, 115−117.

47. Stromstedt, M., Rozman, D., and Waterman, M. R. (1996) The ubiquitously expressed human CYP51 encodes lanosterol 14 alpha-demethylase, a cytochrome P450 whose expression is regulated by oxysterols, *Arch. Biochem. Biophys. 329*, 73−81.

48. Bellamine, A., Mangla, A. T., Dennis, A. L., Nes, W. D., and Waterman, M. R. (2001) Structural requirements for substrate recognition of *Mycobacterium tuberculosis* 14 alpha-demethylase: implications for sterol biosynthesis, *J. Lipid. Res. 42*, 128−136.

49. Aoyama, Y., and Yoshida, Y. (1991) Different substrate specificities of lanosterol 14a-demethylase (P-45014DM) of *S.cerevisiae* and rat liver for 24-methylene-24,25-dihydrolanosterol and 24,-25-dihydrolanosterol, *Biochem. Biophys. Res. Commun. 178*, 1064−1071.

50. De Caprio, J., Yun, J., and Javitt, N. B. (1992) Bile acid and sterol solubilization in 2-hydroxypropyl-beta-cyclodextrin, *J. Lipid Res. 33*, 441−443.

51. Karuppiah, N., and Sharma, A. (1995) Cyclodextrins as protein folding aids, *Biochem. Biophys. Res. Commun. 211*, 60−66.

52. Pikuleva, I. A., Puchkaev, A., and Bjorkhem, I. (2001) Putative helix F contributes to regioselectivity of hydroxylation in mitochondrial cytochrome P450 27A1, *Biochemistry 40*, 7621−7629.

53. Gotoh, O. (1992) Substrate recognition sites in cytochrome P450 family 2 (CYP2) proteins inferred from comparative analyses of amino acid and coding nucleotide sequences, *J. Biol. Chem. 26*, 83−90.

54. Coppens, I., and Courtoy, P. J. (2000) The adaptative mechanisms of *Trypanosoma brucei* for sterol homeostasis in its different life-cycle environments, *Annu. Rev. Microbiol. 54*, 129−156.

55. Hannaert, V., Saavedra, E., Duffieux, F., Szikora, J. P., Rigden, D. J., Michels, P. A., and Opperdoes, F. R. (2003) Plant-like traits associated with metabolism of *Trypanosoma* parasites, *Proc. Natl. Acad. Sci. U.S.A. 100*, 1067−1071.

56. Buckner, F. S., Griffin, J. H., Wilson, A. J., and Van Voorhis, W. C. (2001) Potent anti-*Trypanosoma cruzi* activities of oxidosqualene cyclase inhibitors, *Antimicrob. Agents Chemother. 45*, 1210−1215.

57. Haughan, P. A., Chance, M. L., and Goad, L. J. (1995) Effects of an azasterol inhibitor of sterol 24-transmethylation on sterol biosynthesis and growth of *Leishmania donovani* promastigotes, *Biochem. J. 308*, 31−38.

58. Lira, R., Contreras, L. M., Rita, R. M., and Urbina, J. A. (2001) Mechanism of action of anti-proliferative lysophospholipid analogues against the protozoan parasite *Trypanosoma cruzi*: potentiation of in vitro activity by the sterol biosynthesis inhibitor ketoconazole, *J. Antimicrob. Chemother. 47*, 537−546.

59. Urbina, J. A., Concepcion, J. L., Montalvetti, A., Rodriguez, J. B., and Docampo, R. (2003) Mechanism of action of 4-phenoxyphenoxyethyl thiocyanate (WC-9) against *Trypanosoma cruzi*, the causative agent of Chagas' disease, *Antimicrob. Agents. Chemother. 47*, 2047−2050.

60. Haughan, P. A., and Goad, L. J. (1991) Lipid Biochemistry of Trypanosomatids, in *Biochemical Protozoology* (Coombs, G., North, M., Eds.) pp 312−328, Taylor & Francis, London.